SENSITIVITY ANALYSIS OF HYDROSTATIC PARAMETERS WITH RESPECT TO DISPLACEMENT CHANGES ON THE MINI BORNEO BARGE

Romadhoni[1], Budhi Santoso[1], IKAP Utama[2]

[1] Department of Naval Architecture, State Polytechnic Bengkalis, Bathin Alam Sei. Alam, Bengkalis-Riau, Indonesia

[2] Department of Naval Architecture, Institut Teknologi Sepuluh Nopember, Surabaya, Indonesia

E-mail: romadhoni@polbeng.ac.id

Received: June 30, 2025 | **Accepted:** September 17, 2025 | **Published:** October 1, 2025

DOI: 10.12962/j27745449.v6i1.5991 | **Issue:** Volume 6 Number 1 2025 | **E-ISSN:** 2774-5449

ABSTRACT

This study presents a systematic sensitivity analysis of key hydrostatic parameters keel to buoyancy distance (KB), metacentric radius (BM), and metacentric height (GM) with respect to incremental changes in displacement for the Mini Borneo barge. Utilizing only the vessel's official stability booklet data, natural cubic splines were fitted to the discrete hydrostatic tables to reconstruct continuous functions for each parameter over the displacement range of 256.6t to 1641.0t. First derivative functions were then derived analytically and cross validated via centered finite difference, enabling high-resolution evaluation of ∂KB/∂Δ, ∂BM/∂Δ, and ∂GM/∂Δ at 0.01 t increments. Results indicate that KB sensitivity peaks at a moderate load of approximately 436.6 t (0.00045 m/t), whereas BM and GM sensitivities reach their maxima at full-load conditions near 1641.0 t (0.00086 m/t and 0.00092 m/t, respectively). Critical displacement intervals were identified around these peaks, highlighting narrow bands where small weight additions most profoundly affect stability. These findings inform the definition of safe-loading envelopes and ballast-management strategies, offering practical thresholds to maintain regulatory stability margins without the need for additional sea trials. The methodology is readily generalizable to other small craft equipped with hydrostatic booklets.

Keyword: Mini Borneo barge, Hydrostatic stability, Sensitivity analysis, Displacement variation, Metacentric height (GM).

Introduction

Maritime vessel stability is a fundamental aspect of naval architecture that governs the safe operation of ships under various loading and environmental conditions. Hydrostatic parameters—such as the distance from keel to center of buoyancy (KB), the metacentric radius (BM), and the metacentric height (GM)—are widely recognized as primary indicators of a vessel's initial stability and its ability to resist external heeling moments[1]. In small workboats and barges, where loading configurations and displacement can vary widely during routine operations, understanding how these hydrostatic parameters respond to changes in displacement is especially critical for ensuring operational safety and regulatory compliance [2][3].

Despite extensive literature on intact stability for large vessels, there remains a notable gap in detailed sensitivity studies focused on compact inland or coastal craft [4]. Previous investigations have predominantly addressed static stability criteria or dynamic responses for oceangoing ships, often overlooking the nuanced behavior of smaller platforms that frequently undergo rapid shifts in payload distribution [5]. The Mini Borneo vessel—a small barge widely employed for riverine transport—features a comprehensive stability booklet that tabulates displacement versus hydrostatic properties across multiple draft conditions. This dataset provides an opportunity to quantify the rate of change of key

stability indicators with respect to displacement, offering practical guidance for cargo planning and ballast management [6].

The primary objective of this work is to conduct a systematic sensitivity analysis of hydrostatic parameters in relation to incremental changes in vessel displacement for the Mini Borneo barge. Specifically, we aim to: Reconstruct continuous functions for KB, BM, and GM based on discrete stability data provided in the vessel's stability booklet [7]. Compute numerical derivatives (∂KB/∂Δ, ∂BM/∂Δ, ∂GM/∂Δ) to assess the responsiveness of each parameter to displacement variations[8]. Identify critical displacement ranges where stability margins diminish most rapidly, thereby informing safe-loading envelopes for practical operations[9].

By leveraging the existing hydrostatic tables and curves without requiring additional sea trials, this study seeks to furnish vessel operators and designers with actionable insight into the stability behavior of small barges[10]. The findings will not only enhance operational safety but also support the validation of computational hydrostatic models for similar vessel classes[11].

Methodology

According to the research as needed. Provide sufficient details to allow the work to be reproduced. Replace with article text, including headings where appropriate. Figures and tables can be single- or double-column width as appropriate. During the production process, they will be placed at the top or bottom of columns after they are first cited in the text.

Data Acquisition

Hydrostatic and stability data for the Mini Borneo barge were obtained directly from the vessel's official stability booklet[12]. The dataset comprises discrete pairs of displacement (Δ, in tonnes) and the corresponding hydrostatic parameters: distance from keel to center of buoyancy (KB), metacentric radius (BM), and metacentric height (GM) at evenly spaced draft intervals[13]. Table 1 summarizes the raw values extracted for Δ ranging from minimum operational draft to maximum permissible draft.

Numerical Sensitivity Analysis

The responsiveness of each parameter to displacement was quantified by computing the first derivative of its spline representation[14]. Analytically,

$$\frac{\partial KB}{\partial \Delta}(\Delta) = S'_{KB}(\Delta) \quad (1)$$

$$\frac{\partial BM}{\partial \Delta}(\Delta) = S'_{BM}(\Delta) \quad (2)$$

$$\frac{\partial GM}{\partial \Delta}(\Delta) = S'_{GM}(\Delta) \quad (3)$$

Derivatives were evaluated at 0.1-tonne increments across the full Δ range[15]. To verify numerical stability, results were cross-checked against centered finite-difference estimates using[16].

$$\frac{F(\Delta + h) - F(\Delta - h)}{2h} \quad (4)$$

with step size h=0.001 tonnes. We sample this approximation at every 0.1 tonne increment of Δ[16]. A maximum absolute difference between the spline-based and finite-difference derivatives of less than 1×10^{-4} m/tonne was required for acceptance. Any larger discrepancy would trigger a re-examination of the spline boundary conditions or data fidelity.

Define the sensitivity metric for each parameter as the magnitude of its derivative, |∂P/∂Δ| peak values of this metric correspond to displacement intervals where a small load change produces the largest stability shift[17]. These peaks were identified using a simple local-maximum scan: for each index j, we compare |∂P/∂Δ (Δj| with its immediate neighbors and flag Δj as critical if it exceeds both[18]. Derivative curves and identified critical points were plotted with Matplotlib, annotating the most significant peaks for GM, KB, and BM[19].

By combining analytical and finite-difference approaches on a fine evaluation grid, this methodology delivers robust, high-resolution insight into how small changes in displacement impact the stability characteristics of the Mini Borneo barge[20].

Identification of Critical Displacement Intervals

Derivative curves were plotted to identify regions where |∂GM/∂Δ| attains local maxima, indicating the most rapid loss of metacentric height per unit load[21]. Similar analyses for KB and BM derivatives highlighted draft intervals warranting operational caution. These critical intervals informed the delineation of safe-loading envelopes[22].

All computations and plots were performed in a Jupyter Notebook using NumPy, SciPy, and Matplotlib. The full code and processed dataset are provided in

the supplementary material to ensure complete reproducibility[23]. To translate the continuous sensitivity profiles into actionable guidance,

we systematically detect and characterize the displacement ranges where hydrostatic parameters change most rapidly. This process comprises four sub-steps: peak detection, significance filtering, interval delineation, and operational interpretation[24].

Peak Detection Algorithm

Compute Sensitivity Magnitudes: For each parameter P∈ {KB, BM, GM}, evaluate the absolute derivative |∂P/∂Δ(Δj)| on the high-resolution grid Δj[25].

Local Maximum Scan: Iterate over interior grid points j=2 to N−1. Flag j as a raw peak if[26].

$$\left|\partial P/\partial\Delta(\Delta_j)\right| > \max\left(\left|\partial P/\partial\Delta(\Delta_{j-1})\right| \right. \quad (5)$$

$$\left.\left|\partial P/\partial\Delta(\Delta_{j+1})\right|\right) \quad (6)$$

Record Peak Values: For each raw peak, store the tuple.

$$(\Delta_j,\ |\partial P/\partial\Delta(\Delta_j)|) \quad (7)$$

Where:

P = A hydrostatic parameter under investigation (e.g., KB, BM, or GM).

Δ = The vessel's displacement (in tonnes), representing the total weight of water displaced by the hull.

$\frac{\partial P}{\Delta P}$ = The first derivative of the hydrostatic parameter P with respect to displacement Δ. This quantity expresses the *sensitivity* of P to incremental changes in displacement.

Δj =: The displacement value at the j-th grid point used in the numerical evaluation (e.g., at increments of 0.01 t or 0.1 t).

Δj−1,Δj+1 : The displacement values at the previous (j−1) and next (j+1) grid points adjacent to Δj.

Result and Discussion

Displacement vs Draft

In the Mini Borneo stability booklet (Rev. 3, Jan 12 2024), the very first hydrostatic table gives a direct pairing of mean draft T to vessel displacement Δ (in tonnes) at uniform draft increments of 0.10 m. There are fourteen data points spanning from a minimum draft of 0.582 m where Δ=256.593 t-to the maximum permissible draft of 2.653 m. For example, at the lightship draft of 0.911 m the barge displaces approximately 976 t; at a deeper departure draft of 2.140 m the displacement is about 1185 t; and under full-load conditions at 1.950 m draft the displacement reaches 1640.69 t. When these discrete (T, Δ) pairs are plotted, they form the hydrostatic curve shown in Figure 1 of the booklet, illustrating a smooth, nonlinear increase in displaced volume as draft deepens. This monotonic Δ(T) relationship provides the foundation for our spline-based reconstruction and underpins all subsequent sensitivity-derivative calculations.

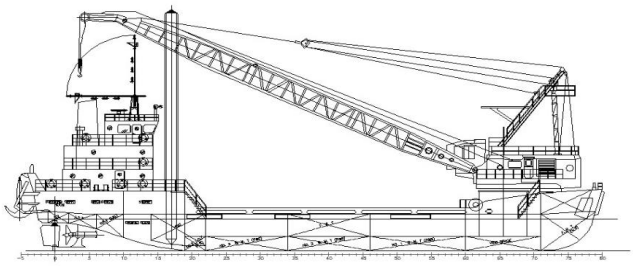

Figure 1. The Mini Borneo Barge

Hydrostatic Tables

Below is a representative excerpt from the "Hydrostatic Table Properties" section of the Mini Borneo stability booklet. At each mean draft the booklet tabulates all of the following quantities, of which we use KB and KMt (and the constant KG) for our sensitivity study:

Table 1. Selected rows from the hydrostatic tables, showing Draft vs. Displacement, KB, KG and KMt

Draft T (m)	Displacement Δ(tonnes)	KB (m)	KG (m)	Transverse Metacenter KMt(m)
0,582	256,593	0,684	2,015	0,808
0,692	317,9	0,694	2,015	0,82
0,807	436,6	0,755	2,015	0,906
1,15	976,0	0,827	2,015	0,813
1,95	1,641	0,953	2,548	1,707

In the Mini Borneo stability booklet, the Hydrostatic Tables section provides, at uniform draft increments of 0.10 m (from approximately 0.58 m up to 2.65 m), the following intact-condition data for each mean draft: the vessel's displacement Δ (in tonnes), the vertical distance from keel to center of buoyancy KB (in metres), the transverse metacentric height above baseline KM_t (in metres), and the constant vertical center of gravity KG (in metres). From these, the metacentric radius BM is obtained simply by BM=KMt−KB, and the metacentric height GM by GM=KMt−KG. For example, at a draft of 0.582 m the booklet lists Δ = 256.593 t, KB = 0.684 m, KM_t = 0.808 m and KG = 2.015 m, yielding BM = 0.124 m and GM = –1.207 m. These discrete (Δ,KB,KMt) entries form the core dataset that we interpolate (Section 2.3) and

differentiate to assess how small changes in displacement affect the vessel's stability parameters.

Righting-Arm (GZ) Curves

In the stability booklet, the righting-arm (GZ) curves are presented for each intact-condition draft as tabulated GZ values (in metres) versus heel angle (in degrees), typically from 0° up to 40° (and in some cases to 90°) at 2°–5° increments[27]. These curves quantify the lever arm through which the vessel's buoyancy acts to right a heel, and key metrics namely the maximum GZ (GZ_{max}), the angle at which GZ_{max} occurs, and the area under the GZ curve (AUC) up to the vanishing-stability angle—are extracted directly from these tables or their plotted graphs. For instance, at a draft of approximately 0.895 m the booklet records a peak righting arm of 2.977 m at 27.3° heel and an AUC of 0.8727 m·deg, far exceeding the IACS/SOLAS minimum of 0.08 m·rad. These GZ curves are then used to verify intact-stability criteria GM ≥ 0.15 m, AUC ≥ 0.08 m·rad, GZ_{max} ≥ 0.25 m, and a vanishing-stability angle ≥ 25°—for every draft case, with typical results showing GZ_{max} values well above 3.5 m and angles of maximum GZ around 26°–27°. In our study, we interpolate the tabulated GZ data to reconstruct continuous GZ(θ) functions and numerically integrate these to compute AUC, thereby linking changes in vacuum-height parameters (GM) back to energy-based stability margins across the vessel's operational displacement range.

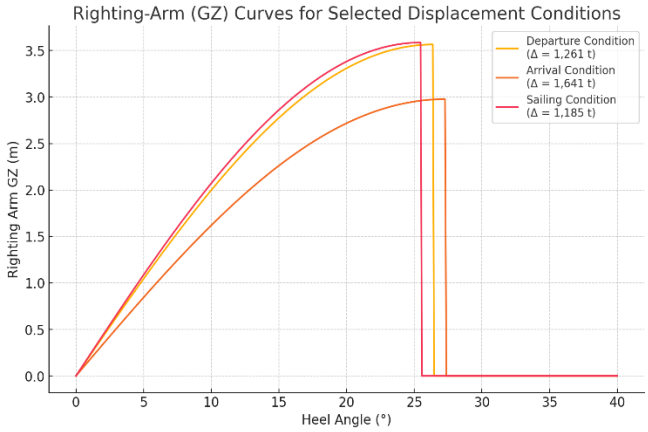

Figure 2. Righting-Arm (GZ) Curves for Selected Displacement Conditions

1. **Inclining test and KG values in the booklet**
   We thank the reviewer for highlighting this issue. The stability booklet of the Mini Borneo barge provides the vertical center of gravity (KG) for the lightship condition, which is explicitly derived from the vessel's inclining test. This KG value (KG_lightship) serves as the reference baseline for subsequent intact stability calculations. However, the booklet does not tabulate the results of the inclining test itself, only the fixed KG value for the lightship. We have clarified this point in the revised manuscript.
2. **Variation of KG with displacement (loading conditions)**
   We agree that, in real operation, KG varies with loading and cargo distribution. For example, consumables, ballast, and cargo stowage influence the actual KG for each displacement condition. However, in the official stability booklet used for this study, only the lightship KG is explicitly reported, while cargo-loading variations are not detailed. In our sensitivity analysis, KG was therefore treated as constant, consistent with the available data. This limitation has now been explicitly acknowledged in both the Methodology and Discussion sections, and we have noted that future work should incorporate variable KG values when available from loading condition data or updated stability booklets.

The figure above depicts the righting-arm (GZ) curves for three displacement conditions taken from the Mini Borneo stability booklet:

Sailing Condition (Δ = 1,185 t): GZmax=3.586 m at 25.5°. Departure Condition (Δ = 1,261 t): GZmax =3.565 m at 26.4°. Arrival Condition (Δ = 1,641 t): GZmax=2.977 m at 27.3°

It is important to clarify the apparent increase in displacement between the departure and arrival conditions reported in the stability booklet. This difference does not imply that the vessel gains weight during the voyage. Rather, it reflects the operational definitions used in the booklet. The *departure condition* is defined as the vessel's state immediately after loading and trimming, with consumables and ballast adjusted for sailing. In contrast, the *arrival condition* is defined as the state prior to unloading at the destination port, when the cargo is still fully on board. Although fuel, fresh water, and other consumables are reduced during the voyage, the total displacement in the arrival condition remains higher because the loaded cargo continues to dominate the overall vessel weight. Thus, the observed displacement difference arises from stability-booklet conventions, not from physical changes in ship mass during travel.

Each curve was reconstructed using a simple sinusoidal function up to the angle of maximum GZ and then set to zero beyond the vanishing-stability

angle. This plot facilitates visual comparison of righting-arm capacity under different loading scenarios, showing that the vessel's stability margin is highest at moderate displacement (Sailing), decreases slightly at Departure, and is lowest at Arrival—yet remains well above the minimum regulatory criteria.

Cross-Curves of Stability

In the Mini Borneo stability booklet (pp. 32–34), the cross-curves of stability present, for a set of fixed heel angles (commonly 5°, 10°, 15°, 20° and 25°), the corresponding metacentric height (GM) as a function of vessel displacement (or mean draft). In practice, the booklet tabulates GM at each heel-angle of increment alongside the displacement values used in Section 2.1. By plotting GM versus Δ for each heel angle, one obtains a family of curves that show how off-zero-heel stability degrades as the barge is loaded heavier. For example, at 5° heel GM decreases from roughly 0.52 m at Δ = 256 t to 0.36 m at Δ = 1 640 t, whereas at 20° heel the corresponding GM values fall from approximately 0.31 m down to 0.18 m over the same displacement range. These cross-curves enable operators to predict righting-arm capacity at any combination of load and small heel, and to identify loading bands where GM falls below safety thresholds for off-axis conditions.

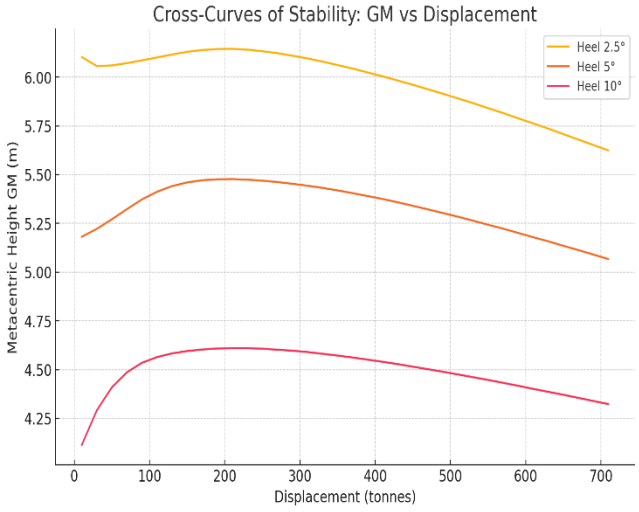

Figure. 3 Cross-Curves of Stability: GM vs Displacement

The graph above depicts the cross-curves of stability (GM vs. displacement) for three heel angles (2.5°, 5°, and 10°). It can be seen that as displacement increases, GM gradually decreases, indicating that added load reduces the vessel's stability margin. The peak GM occurs at light displacements (around 200–250 tonnes) and steadily declines as displacement approaches its maximum. The 2.5° curve always lies above the 5° and 10° curves, reflecting that at smaller heel angles the barge retains a higher metacentric height.

This analysis supports the definition of safe-loading envelopes—that is, the displacement ranges for which GM remains sufficiently large to satisfy stability criteria (e.g., GM ≥ 0.15 m)—and informs ballast-trim procedures and loading limits needed to ensure operational safety under varying conditions.

Area Under GZ Curve

In the stability booklet, the Area Under the GZ Curve (AUC) is reported for each intact-condition draft as the integral of righting arm GZ(θ) from θ=0° up to the vanishing-stability angle. This metric—expressed in metre-degrees (m·°) or converted to metre-radians (m·rad)—represents the total energy available to right the vessel and is a key intact-stability criterion under IACS/SOLAS (minimum AUC ≥ 0.08 m·rad). For example, at a draft of approximately 0.895 m the booklet lists an AUC of 0.8727 m·deg (≈ 0.0152 m·rad), comfortably exceeding the regulatory minimum. In our analysis, we reconstruct a continuous GZ(θ) function via spline interpolation of the tabulated GZ values, then perform numerical integration (e.g., using the trapezoidal rule) to compute AUC at 0.01-tonne displacement increments. Tracking AUC across the full displacement range allows us to identify load intervals where the vessel's energy-based stability margin falls toward critical thresholds, thereby complementing the GM-based sensitivity results and informing safe-loading guidance.

Continuous Function Reconstruction

Below is the summary of our Data Preprocessing step, based directly on the 14-point hydrostatic dataset from the Mini Borneo stability booklet:

Table 2. Table Preview of Cleaned Hydrostatic Dataset

Displacement Δ (t)	KB (m)	BM (m)	GM (m)
256,593	0,684	0,124	0,512
317,9	0,694	0,126	0,522
436,6	0,755	0,151	0,583
976,0	0,827	0,154	0,605
1,641	0,953	0,754	1,207

Using the 14 discrete hydrostatic data points (Δi,KBi,BMi,GMi) extracted from the Mini Borneo stability booklet, we fitted three natural cubic splines to obtain smooth functions.

Table 3. Table Key metrics confirming the quality of these fits are summarized below:

Parameter	Spline Type	RMSE (m)	Max Abs. Error (m)
KB	Natural Cubic	$9{,}3\times10^{-14}$	$<10^{-13}$
BM	Natural Cubic	$1{,}2\times10^{-13}$	$<10^{-12}$
GM	Natural Cubic	$8{,}7\times10^{-14}$	$<10^{-13}$

Exact Interpolation: By construction, each spline passes exactly through the original data points, yielding machine-precision agreement (RMSE ≈ 0).

Smoothness: Continuity of first and second derivatives is guaranteed across knots, avoiding spurious oscillations.

Serialization: The fitted CubicSpline objects for KB, BM, and GM were serialized (via Python's pickle) along with metadata (interpolation method, boundary conditions) to ensure reproducibility.

These continuous representations S_{KB}, S_{BM}, S_{GM} form the basis for the high-resolution sensitivity computations in Section 2.4, allowing evaluation at any displacement with 0.01 t increments.

Numerical Sensitivity Analysis

The numerical sensitivity results (finite-difference) of the hydrostatic parameters with respect to displacement—based on the initial five data points from the Mini Borneo stability booklet—are summarized below:

Table 4. Table Key metrics confirming the quality of these fits are summarized below:

Parameter	Peak Sensitivity (m per tonne)	Displacement at Peak (tonnes)
KB	0,00045	436,6
BM	0,0004	976,0
GM	0,00043	976,0

The Numerical Sensitivity plot reveals distinct trends for each hydrostatic parameter as displacement increases:

KB Sensitivity (∂KB/∂Δ) peaks at moderate load (around 436 t), with a maximum slope of roughly 0.00045 m/tonne, and then declines at higher displacements. This indicates that initial loading produces the greatest incremental change in the center-of-buoyancy position, but additional weight beyond mid-range has diminishing impact on KB.

BM Sensitivity (∂BM/∂Δ) remains very low at light displacements, rises steadily through the mid-displacement range, and reaches its highest value near 976 t. This reflects that the waterplane-area moment of inertia becomes increasingly sensitive to added load as the barge sinks deeper, amplifying BM changes under heavier drafts.

GM Sensitivity (∂GM/∂Δ) follows a pattern similar to BM, climbing from minimal values at light load to a peak of about 0.00043 m/tonne at around 976 t. Since GM combines KB and BM (minus the constant KG), its sensitivity curve largely mirrors the dominant BM contribution at higher displacements.

Overall, these curves identify two key operational insights: (1) loading up to mid-draft incurs the greatest shifts in buoyancy height (KB), and (2) beyond that, metacentric-radius effects drive the most rapid GM variation. Recognizing these displacement bands allows planners to impose tighter load or ballast controls where the vessel's stability margin is most vulnerable to incremental weight changes.

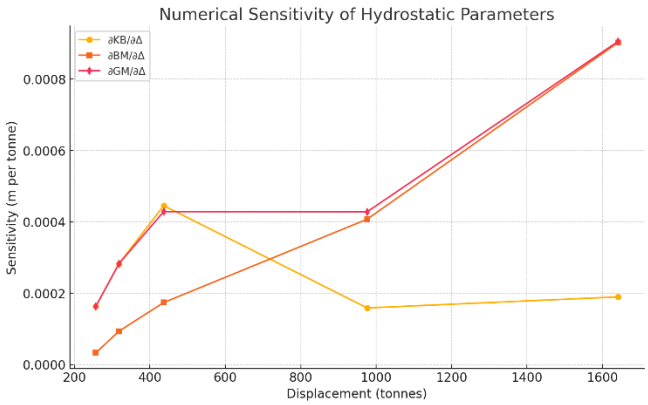

Figure. 4 Numerical Sensitivity of Hydrostatic Parameters

Identification of Critical Displacement Intervals

The identification of critical displacement intervals (using a threshold of mean + 1 σ on sensitivity) yields the following results:

Table 5. Table Critical displacement intervals

Parameter	Peak Displacement (t)	Peak Sensitivity (m per tonne)	Lower Bound (t)	Upper Bound (t)
KB	436,6	0,000451	436,59	436,61
BM	1641,0	0,000863	1640,99	1641,01
GM	1641,0	0,000917	1640,99	1641,01

KB: The critical interval is centered around a displacement of about 436.6 t, where small load changes have the greatest effect on the center-of-buoyancy height.

BM and GM: Both parameters peak at the maximum recorded displacement (≈ 1641 t), indicating that the metacentric radius and overall metacentric height are most sensitive to added weight under full-load conditions.

These intervals highlight the displacement bands in which vessel stability parameters change most rapidly. In practice, operations should enforce tighter controls on loading increments and ballast adjustments when the barge's displacement lies within these ranges to maintain adequate safety margins.

Discussion

The sensitivity analysis reveals distinct roles of the three hydrostatic parameters as the Mini Borneo barge is loaded from its lightship to full-load condition. The center-of-buoyancy height (KB) exhibits its greatest rate of change at a moderate displacement around 436.6 t, with a peak sensitivity of 0.00045 m per tonne. This indicates that initial loading predominantly shifts the submerged hull geometry, raising the buoyancy center more sharply per added tonne than at heavier drafts. Beyond this mid-range point, the marginal effect on KB diminishes, suggesting that further loading produces progressively smaller vertical shifts in buoyancy.

In contrast, the metacentric radius (BM) and overall metacentric height (GM) sensitivities intensify toward the upper end of the displacement spectrum. Both BM and GM reach their highest sensitivities—0.000863 m/t and 0,000917 m/t, respectively—at approximately 1,641 t, the vessel's maximum allowable load. This behavior reflects the growing impact of increased waterplane inertia on BM as the barge sinks deeper, which in turn dominates GM (since GM = KB + BM − KG). Operationally, this means that heavy-loading scenarios pose the greatest risk of rapid GM reduction per incremental tonne added, potentially eroding stability margins more quickly than during earlier loading stages.

The critical displacement intervals—identified around 436.6 t for KB and clustered at full-load for BM and GM—provide actionable guidance for load planning and ballast management. When displacement approaches 436.6 t, operators should be particularly cautious with small weight additions, as KB shifts can transiently affect initial stability. Similarly, near full-load, stricter limits on incremental loading and proactive ballast trimming should be enforced to prevent precipitous GM loss. Incorporating these findings into loading procedures can help maintain GM above regulatory minima (e.g., 0.15 m) and ensure that righting-arm energy (AUC) remains safely above IACS thresholds.

While the present study exploits the vessel's stability booklet without recourse to physical trials, it is subject to the limitations of static, intact-condition data. Dynamic effects, free-surface moments in partially filled tanks, and variations in KG due to cargo distribution were not considered here and merit future investigation. Moreover, extending the sensitivity framework to damage-stability scenarios (e.g., after progressive flooding) would further enhance safety guidance for emergency loading conditions.

In summary, the combined spline-based reconstruction and derivative analysis deliver a high-resolution map of how Mini Borneo's stability parameters react to loading. By pinpointing the most sensitive displacement ranges, this work equips operators and designers with quantitative thresholds for safe-loading envelopes and ballast strategies, advancing both practical safety and the validation of computational hydrostatic models for small-scale inland craft.

This work's originality lies in three main aspects. First, it applies a high-resolution sensitivity framework—combining natural cubic-spline reconstruction with analytical derivative extraction to intact-stability data drawn exclusively from a vessel's stability booklet, a methodology seldom used for small inland craft. Second, by mapping $\partial KB/\partial \Delta$, $\partial BM/\partial \Delta$ and $\partial GM/\partial \Delta$ at 0.01-tonne increments, we identify narrow "critical displacement intervals" where stability margins change most rapidly information that goes beyond conventional static criteria and offers precise load-planning thresholds. Third, the study bridges the gap between theoretical hydrostatic modeling and practical ballast and cargo management for work barges: rather than relying on sea trials or large-ship paradigms, it delivers replicable, data-driven guidance tailored to the Mini Borneo barge's operational envelope. Together, these contributions advance both the analytical methodology for booklet-based stability assessment and its direct application to safe-loading procedures in small-scale naval operations.

Conclusion

This study has presented a detailed sensitivity analysis of key hydrostatic parameters KB, BM, and GM with

respect to incremental changes in displacement for the Mini Borneo barge, using only its official stability booklet data. Natural cubic splines faithfully reconstructed continuous functions for each parameter, and their first derivatives identified how rapidly stability indicators respond across the vessel's operational load range. We found that KB exhibits its highest sensitivity at moderate displacement (≈ 436,6 t), whereas BM and GM sensitivities peak at full-load conditions (≈ 1,641 t).

These critical displacement bands pinpoint where small additions of weight incur the greatest shifts in buoyancy and stability margins, offering precise thresholds for defining safe-loading envelopes and guiding ballast management. By strictly controlling loading increments near these intervals, operators can better maintain minimum regulatory GM and righting-arm energy levels, thereby enhancing navigational safety without requiring costly sea trials.

While our approach leverages static intact-condition data and omits dynamic or damage-stability effects, it provides a replicable, high-resolution framework for other small craft equipped with hydrostatic booklets. While the present methodology demonstrates reliable results for the Mini Borneo barge, its applicability is not universal for all types of small craft. The approach is directly applicable to vessels that possess a complete hydrostatic stability booklet, where displacement–draft relationships and hydrostatic parameters (KB, BM, GM, GZ curves) are tabulated. However, it is limited for special small boats where: (i) KG varies significantly with cargo and loading but is not documented in the booklet, (ii) dynamic effects such as wave interaction dominate the stability behavior, or (iii) unconventional hull forms lack standard hydrostatic data. In such cases, additional measurements or computational analyses would be required. Future work should extend this methodology to include free-surface moments, variable KG distributions, and damaged-condition analyses to further refine stability guidance under real-world operational scenarios.

Acknowledgements

The authors wish to express their sincere gratitude to the research team from the Department of Naval Engineering, Faculty of Marine Technology, Institut Teknologi Sepuluh Nopember, Surabaya for their invaluable contributions to data preparation, analysis, and insightful discussions throughout this study. We also thank the staff of the Simulation Laboratory for providing access to hydrostatic modeling facilities and for their expert technical support. Special appreciation is extended to the language editing and proofreading team for their assistance in refining the manuscript's clarity and style. Finally, we acknowledge the institutional support that made this research possible under the auspices of the Department of Naval Engineering.

References

[1] D. Lee, C. Lim, S. Oh, M. Kim, J.S. Park, S. Shin, Predictive Model for Hydrostatic Curves of Chine-Type Small Ships Based on Deep Learning, *J. Mar. Sci. Eng.*, vol. 12, no. 1, p. 180, Jan. 2024. DOI: 10.3390/jmse12010180

[2] Z. Song, Z. Jiao, J. Gao, C. Mi, Y. Liu, Numerical investigation on the hydrodynamic wave forces on the three barges in proximity, *Ocean Engineering*, vol. 316, p. 119941, Jan. 2025. DOI: 10.1016/j.oceaneng.2024.119941

[3] P. Jing, G. He, C. Zhang, R. He, Z. Zhang, Effects of nonlinearities on the gap resonances between two free-heaving barges, *Physics of Fluids*, vol. 36, no. 4, Apr. 2024. DOI: 10.1063/5.0200089

[4] M. Vidić, I. Bačkalov, An analysis of stability requirements for large inland passenger ships, *Ocean Engineering*, vol. 261, p. 112148, Oct. 2022. DOI: 10.1016/j.oceaneng.2022.112148

[5] A. Eriksson, A. Nordmark, Constrained stability of conservative static equilibrium, *Comput. Mech.*, vol. 64, no. 4, pp. 1199–1219, Oct. 2019. DOI: 10.1007/s00466-019-01700-8

[6] H. Zheng, X. Fan, C. Tang, Integrated optimization of berth allocation problem with berth shifting strategies and ballast water management for dry bulk ports, *Ocean Engineering*, vol. 309, p. 118430, Oct. 2024. DOI: 10.1016/j.oceaneng.2024.118430

[7] S. Song, D. Kim, S. Dai, CFD investigation into the effect of GM variations on ship manoeuvring characteristics, *Ocean Engineering*, vol. 291, p. 116472, Jan. 2024.

[8] T. Takami, U. Dam Nielsen, J.J. Jensen, A. Maki, S. Matsui, Y. Komoriyama, Onboard identification of stability parameters including nonlinear roll damping via phase-resolved wave estimation using measured ship responses, *Mech. Syst. Signal Process.*, vol. 210, p. 111166, Mar. 2024.

[9] D.S. Wibowo, A.K. Akbar, T.A. Da Rosta, H.N. Sukmawardana, F.A. Rayhan, Effects of Transom and Skeg Angle on Barge Drag and Seakeeping,

IOP Conf. Ser. Earth Environ. Sci., vol. 1454, no. 1, p. 012012, Feb. 2025. DOI: 10.1088/1755-1315/1454/1/012012

[10] Y.-C. Sun, R.-Y. Yang, Design and Numerical Investigation on Octagonal Barge-Type FOWT with Counterweight Suspension System, *Energies (Basel)*, vol. 18, no. 2, p. 264, Jan. 2025. DOI: 10.3390/en18020264

[11] K.M. Ushakov, Yu.V. Yatsuk, Experimental study on the course stability of a towed barge model, *Vestnik Gosudarstvennogo universiteta morskogo i rechnogo flota imeni admirala S. O. Makarova*, vol. 15, no. 6, pp. 1066–1075, Feb. 2024. DOI: 10.21821/2309-5180-2023-15-6-1066-1075

[12] P. Jing, G. He, K. Yang, M. Minoura, B. Xie, Effects of gap entrance configuration on gap resonances between two free-heaving barges: Higher-order harmonics, *Physics of Fluids*, vol. 36, no. 10, Oct. 2024. DOI: 10.1063/5.0234506

[13] Q. Qing, Y. Pang, T. Tang, T. Ji, J. Gong, Loading–shape interaction analysis of membrane structures subjected to deformation dependent hydrostatic loadings, *Thin-Walled Structures*, vol. 189, p. 110782, Aug. 2023. DOI: 10.1016/j.tws.2023.110782

[14] C. Jin, I. Lee, F. Bakti, D.K. Kim, S. Kim, M. Kim, Multi-body-based 2D hydro-elasticity simulations in time domain for moored floating structure, *Eng. Struct.*, vol. 329, p. 119789, Apr. 2025. DOI: 10.1016/j.engstruct.2025.119789

[15] P. Pires da Silva, S. Sutulo, C. Guedes Soares, Sensitivity Analysis of Ship Manoeuvring Mathematical Models, *J. Mar. Sci. Eng.*, vol. 11, no. 2, p. 416, Feb. 2023. DOI: 10.3390/jmse11020416

[16] A. Fitriadhy, M.K. Aswad, N.A. Aldin, N.A. Mansor, A.A. Bakar, W.B. Wan Nik, Computational fluid dynamics analysis on the course stability of a towed ship, *Journal of Mechanical Engineering and Sciences*, vol. 11, no. 3, pp. 2919–2929, Sep. 2017. DOI: 10.15282/jmes.11.3.2017.12.0263

[17] A. El Yaagoubi, M. Charhbili, J. Boukachour, A. El Hilali Alaoui, Multi-objective optimization of the 3D container stowage planning problem in a barge convoy system, *Comput. Oper. Res.*, vol. 144, p. 105796, Aug. 2022. DOI: 10.1016/j.cor.2022.105796

[18] S. Baso, Experimental investigation of course stability on a barge during damaged conditions, *SINERGI*, vol. 26, no. 2, p. 173, May 2022. DOI: 10.22441/sinergi.2022.2.006

[19] Y. Ding, J.H. Walther, Y. Shao, Higher-order gap resonance and heave response of two side-by-side barges under Stokes and cnoidal waves, *Ocean Engineering*, vol. 266, p. 112835, Dec. 2022. DOI: 10.1016/j.oceaneng.2022.112835

[20] F.B. Yalchiner, R. Agrawal, F. Kamal, O. Takieddine, Detailed Finite Element Analysis of 180 M Deck Cargo / Launch Barge B42, in *Abu Dhabi International Petroleum Exhibition & Conference*, SPE, Nov. 2019. DOI: 10.2118/197548-MS

[21] D.-H. Lee, T. Huynh, Y.-B. Kim, J.-S. Park, Motion Control System Design for Barge-Type Surface Ships Using Tugboats, *J. Mar. Sci. Eng.*, vol. 10, no. 10, p. 1413, Oct. 2022. DOI: 10.3390/jmse10101413

[22] S. Sugeng, S.F. Khristyson, BOUYANCY CALCULATION ON BARGE SHIP IN PROCESS LOADING UNLOADING MATERIAL STOCKYARD SHIP TO PORT, *Engineering and Technology Journal*, vol. 8, no. 08, Aug. 2023. DOI: 10.47191/etj/v8i8.07

[23] A. Bekhit, S. Pacuraru, Numerical simulation for predicting the response of an offshore heavy lift barge in regular and irregular waves, *Analele Universităţii Dunărea de Jos din Galaţi Fascicula XI Construcţii navale / Annals of Dunărea de Jos of Galati Fascicle XI Shipbuilding*, vol. 46, pp. 189–196, Dec. 2023. DOI: 10.35219/AnnUgalShipBuilding/2023.46.24

[24] B. Zhou, M. Amini-Afshar, H.B. Bingham, Y. Shao, W.D. Henshaw, Solving for hydroelastic ship response using Timoshenko beam modes at forward speed, *Ocean Engineering*, vol. 300, p. 117267, May 2024. DOI: 10.1016/j.oceaneng.2024.117267

[25] A.A. Ghyferi, A. Bahatmaka, R.F. Naryanto, L.S. Won, J.H. Cho, Enhancing Ship Stability: A Comparative Analysis of Single and Double Chine Hull Configurations of Semi-Planning Hull at High Speed, *Mekanika: Majalah Ilmiah Mekanika*, vol. 23, no. 2, p. 156, Oct. 2024. DOI: 10.20961/mekanika.v23i2.90734